DIGITAL ACCESS TO SCHOLARSHIP AT HARVARD
DASH.HARVARD.EDU

HARVARD LIBRARY
Office for Scholarly Communication

Accurate galactic N(H) values towards quasars and AGN

Citation
Elvis, Martin, Belinda J. Wilkes, and Felix J. Lockman. 1989. "Accurate Galactic N(H) Values Towards Quasars and AGN." The Astronomical Journal 97 (March): 777. doi:10.1086/115022.

Published Version
doi:10.1086/115022

Permanent link
http://nrs.harvard.edu/urn-3:HUL.InstRepos:30212152

Terms of Use
This article was downloaded from Harvard University's DASH repository, and is made available under the terms and conditions applicable to Other Posted Material, as set forth at http://nrs.harvard.edu/urn-3:HUL.InstRepos:dash.current.terms-of-use#LAA

Share Your Story

The Harvard community has made this article openly available.
Please share how this access benefits you. Submit a story .

Accessibility

1989AJ.....97..777E

ACCURATE GALACTIC N_H VALUES TOWARDS QUASARS AND AGN

MARTIN ELVIS
Harvard-Smithsonian Center for Astrophysics, 60 Garden Street, Cambridge, Massachusetts 02138

FELIX J. LOCKMAN
National Radio Astronomy Observatory,[a] Edgemont Road, Charlottesville, Virginia 22903

BELINDA J. WILKES
Harvard-Smithsonian Center for Astrophysics, 60 Garden Street, Cambridge, Massachusetts 02138
Received 18 October 1988

ABSTRACT

We have measured integrated Galactic 21 cm column densities toward ~ 174 quasars and active galactic nuclei using the NRAO 140 ft telescope at Green Bank. These data have been corrected for stray radiation with the technique of Lockman *et al.* (1986). The 21 arcmin beam size of the 140 ft is small enough to minimize the uncertainty in N_H due to angular variations in the H I of the Galaxy at high latitudes. The resulting column densities are accurate to $\sim 1\times 10^{19}$ atoms cm^{-2} or $\sim 5\%$, whichever error is larger. Opacity uncertainties dominate the errors above $N_H \sim 4\times 10^{20}$ atoms cm^{-2}.

I. THE NEED FOR ACCURATE N_H VALUES

The extension of sensitive extragalactic x-ray measurements into the band below the 0.28 keV carbon edge (the "C band," McCammon *et al.* 1983) has made it important to determine accurately the opacity of the interstellar medium of our own galaxy at these energies. Interpretation of spectral results from the *Einstein* IPC (Imaging Proportional Counter, Gorenstein *et al.* 1981) and the *EXOSAT* CMA (Channel Multiplier Array, Taylor *et al.* 1981) depend critically on a knowledge of the Galactic N_H. The inferred properties of the recently discovered "ultrasoft excesses" in the x-ray spectra of quasars and active galactic nuclei (AGN) are particularly sensitive to this value (Wilkes and Elvis 1987; Branduardi *et al.* 1987; Giommi and Tagliaferri 1987).

Most x-ray astronomers currently use the unpublished but widely circulated "Bell Labs" survey (Stark *et al.* 1984) of 21 cm H I emission to determine the column densities of interstellar material toward extragalactic sources. This survey is superior to previous all-sky H I surveys because the telescope's unblocked aperture makes it almost free of "stray radiation" entering the signal from distant sidelobes. The small size of the antenna, however, has the disadvantage that its angular resolution is poor, typically $\sim 2°\times 3°$. Small-scale structure in the H I distribution on the sky is thus liable to introduce errors in the column toward any particular line of sight. Elvis *et al.* (1986, Appendix B) estimated that the 90% errors introduced by small-scale structure were $\pm 1\times 10^{20}$ atoms cm^{-2}. For a typical high Galactic latitude position with $N_H \sim 3\times 10^{20}$ atoms cm^{-2}, this uncertainty of 1×10^{20} atoms cm^{-2} in N_H leads to a factor-of-2.4 uncertainty in the intrinsic x-ray flux density of a source at 0.2 keV. Column densities more accurate than the Bell Labs survey provides are thus clearly needed.

A method for achieving high-angular-resolution H I measurements free from stray radiation has recently been developed for the Green Bank 140 ft telescope (Lockman, Jahoda, and McCammon 1986, Appendix A). We have used this technique to produce accurate H I column densities toward a large number of quasars and AGN that are bright and well-observed x-ray sources. We present these column densities here. We also analyze the results to provide an assessment of the remaining errors and to determine more carefully the uncertainties involved in using the Bell Labs survey values when no more accurate measurement is available.

II. OBSERVATIONS

The sample of objects includes a wide selection of x-ray-observed AGN and quasars. It includes, so far as they were observable from Green Bank (i.e., declination $\gtrsim -40°$), all the quasars with *Einstein* IPC spectra in Wilkes and Elvis (1987), all the BL Lac objects with *Einstein* IPC spectra in Madejski (1985), a substantial number of other *Einstein* observed quasars for which IPC x-ray "colors" are available (Brunner *et al.* 1988), all of the members of the complete hard (2–10 keV) x-ray-selected "Piccinotti" sample of AGN (Piccinotti *et al.* 1982), and a selection of the AGN detected by the Medium Energy instrument on *EXOSAT* (Sternberg *et al.* 1986). In addition, we mapped the accessible *Einstein* Deep Survey regions (Giacconi *et al.* 1979), the "Braccesi" survey region covered by Marshall *et al.* (1984), SA 57, and the North Ecliptic Pole regions that will be observed in depth by *ROSAT*. The maps for these extended regions will be presented separately.

The observing technique was as detailed by Lockman *et al.* (1986, Appendix A). Briefly, the 140 ft telescope is used to map out the beam covered by the Bell Labs observation that was centered closest to the position of each AGN. The 140 ft data are then convolved with the beam profile of the Bell antenna to give the 21 cm spectrum that the 140 ft would observe if it had the same beam shape as the Bell antenna, i.e., including the stray radiation seen by the 140 ft at this position. This spectrum is dependent on the altitude and azimuth of the telescope as well as on the celestial position. The difference between the Bell spectrum and the convolved 140 ft spectrum is then the stray radiation seen by the 140 ft at that position. This is then subtracted from the 140 ft spectrum taken at the precise position of the active galactic nucleus.

[a] The National Radio Astronomy Observatory is operated by Associated Universities, Inc., under contract with the National Science Foundation.

 0004-6256/89/030777-06$00.90 © 1989 Am. Astron. Soc.

© American Astronomical Society • Provided by the NASA Astrophysics Data System

1989AJ.....97..777E

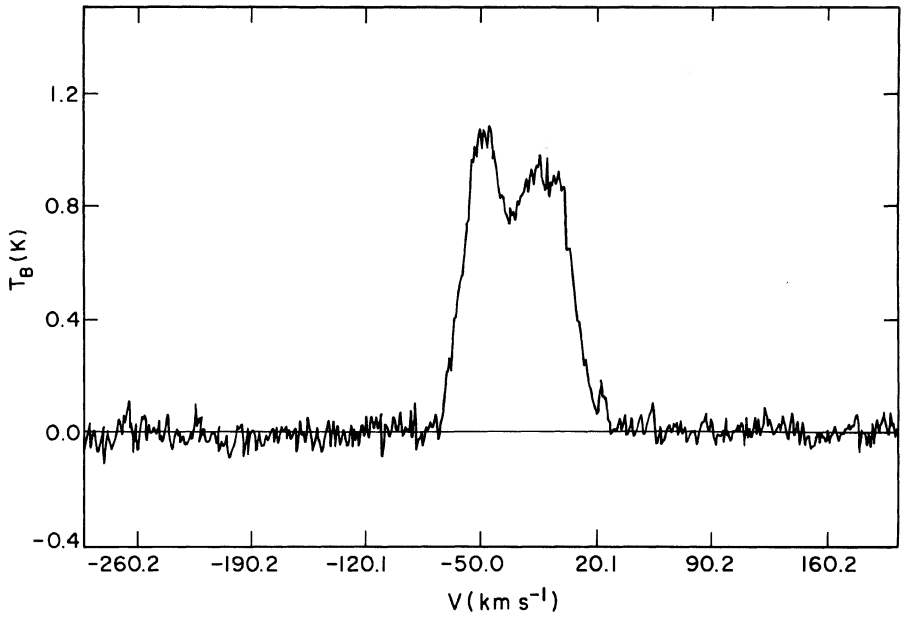

FIG. 1. Low signal-to-noise 21 cm spectrum from the NRAO 140 ft. The N_H in this spectrum (corrected for stray radiation) is 1.23×10^{20} atoms cm^{-2} 1225 + 317).

In practice, two independent spectra were taken at each AGN position. Total integration times were 2–6 min. Because of the low system temperature (18 K at zenith), these integration times are sufficient to make the uncertainty in N_H due to noise negligible. An observation of particularly low signal-to-noise is shown in Fig. 1. Each AGN position was observed both immediately before and after the Bell beam was mapped and the results averaged, to minimize time-dependent effects. Remaining errors in the observation are primarily due to uncertainties in the baseline (Lockman *et al.* 1986) and amount to $\sim2\times10^{18}$ atoms cm^{-2}. The amount of the stray radiation removed was equivalent to H I columns of a few $\times10^{19}$ atoms cm^{-2}, or $\sim15\%$ for typical values of N_H. Figure 2 shows an example of a particularly large stray-radiation spectrum compared with the observed 140 ft spectrum. There is uncertainty in the stray-radiation correction at a level of a few times 10^{18} atoms cm^{-2}, and the form of the uncertainty is not well determined.

To derive an integral N_H measurement from the observed spectrum requires a correction for the opacity τ of the gas. Although at high Galactic latitudes this correction is generally small, it is sometimes dominant. The correction is intrinsically uncertain. The observed spectrum is made up of contributions from different clouds in the interstellar medium, which generally have a wide range of temperatures and optical depths and many possible geometric arrangements (see discussions in Dickey and Benson 1982; Lockman and Dickey 1989). The distribution of these clouds cannot be derived

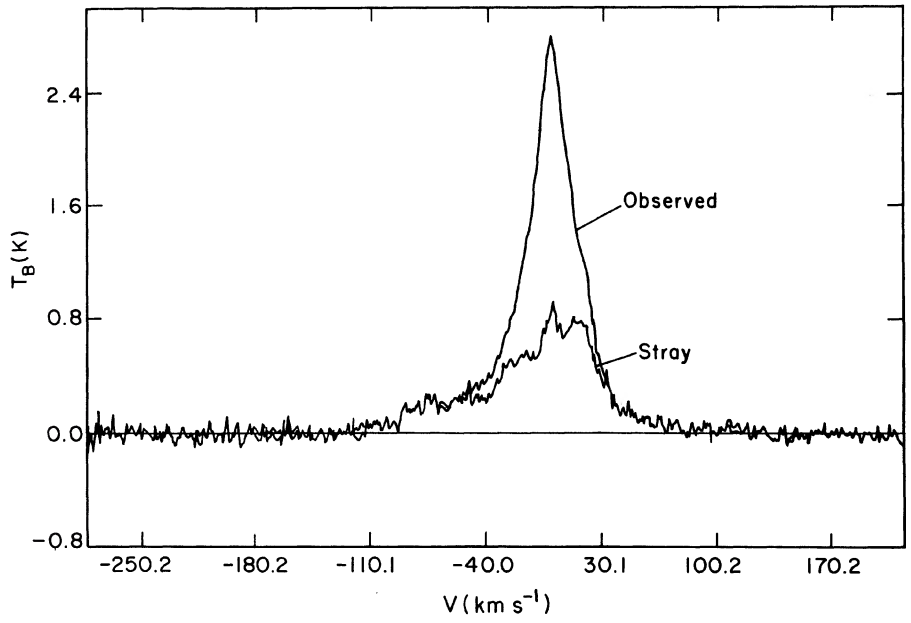

FIG. 2. Sample of the stray-radiation spectrum (lower line) removed from the observed data (upper line).

© American Astronomical Society • Provided by the NASA Astrophysics Data System

1989AJ.....97..777E

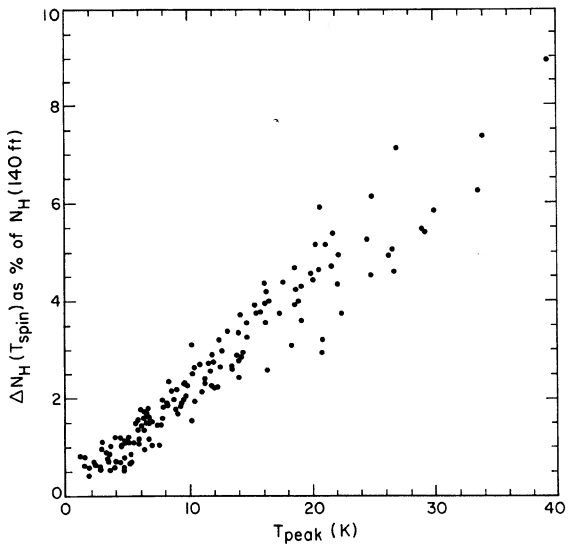

FIG. 3. Uncertainty due to opacity uncertainties (N_H (10 000 K) $- N_H$ (125 K)) as a function of peak brightness temperature (T_{peak}) in the 140 ft spectrum.

from a 21 cm spectrum. The size of the uncertainty can be estimated using the peak observed brightness temperature in the spectrum T_{peak} since

$$T_{peak} = T_{spin}(1 - e^{-\tau}),$$

if we assume that the emission arises from gas of a fixed kinetic temperature (called the spin temperature T_{spin} for historical reasons). If T_{peak} is small, then τ is always small for reasonable values of T_{spin}, but for larger T_{peak}, τ is more likely to be significant and one must make an opacity correction. Figure 3 shows the uncertainty in N_H due to opacity corrections, $\Delta N_H(T_{spin})$, plotted against T_{peak}. $\Delta N_H(T_{spin})$ was calculated using T_{spin} values of 10^4 K and 125 K as extreme cases. A best fit to Fig. 3 gives

$$\Delta N_H(T_{spin}) = (0.073 \pm 0.005)T_{peak} - (0.063 \pm 0.007) \quad (10^{20} \text{ atoms cm}^{-2}).$$

This expression, or Fig. 3, can be used to estimate the opacity-correction uncertainty in our N_H measurements.

The best-estimate column densities are given in Table I. Values of N_H are given for an assumed effective spin temperature of 250 K, which is a good approximation to that of the interstellar H I (Dickey, private communication; see also Dickey 1988). When the H I signal is brighter than several tens of Kelvins, the Bell Labs survey data, and hence our

TABLE I. Galactic column densities toward AGN from Green Bank 140 ft data.

Object	R.A.	decl.	N_H^a	T_{peak}	Notes	Object	R.A.	decl.	N_H^a	T_{peak}	Notes
MCS 18	00 02 46.2	05 07 30	3.87	9.6		H0548-322	05 48 48.9	−32 16 60	2.49	3.9	
PHL658	00 03 25.0	15 53 08	3.94	14.7		NGC2110	05 49 46.3	−07 28 01	18.60	53.4	1
IIIZW2	00 07 56.7	10 41 47	6.09	24.5		MCG8-11-11	05 51 09.7	46 25 51	20.27	39.7	1
3C 9	00 17 50.0	15 24 17	4.02	18.7		H0557-385(A)	05 56 21.0	−38 20 15	3.35	6.6	
PG0026+129	00 26 38.1	12 59 29	4.93	18.6		0642+449	06 42 52.9	44 54 31	11.61	26.2	
0038-020	00 38 23.7	−02 02 51	2.57	5.9		3C 175	07 10 15.9	11 51 26	11.51	26.7	
UM 275	00 43 39.5	00 48 04	2.03	5.6		MKN376	07 10 35.7	45 47 09	9.32	16.3	
PKS0044+030	00 44 31.3	03 03 34	3.00	9.0		PKS0735+17	07 35 14.0	17 49 09	4.35	9.2	
PG0049+171	00 49 16.5	17 09 40	4.26	16.5		0736+017	07 36 42.3	01 44 00	8.91	26.5	
I ZW I	00 50 57.7	12 25 20	5.07	20.3		MKN 79	07 38 46.8	49 55 46	5.89	22.3	
0052+251	00 52 11.1	25 09 24	4.50	13.9		3C 186	07 40 56.9	38 00 32	4.87	9.7	
PHL909	00 54 31.9	14 29 59	4.20	14.0		3C 191	08 02 03.9	10 23 56	2.54	4.7	
0106+013	01 06 04.3	01 19 01	2.63	6.9		PG0804+76	08 04 35.4	76 11 31	3.12	12.2	
MKN1152	01 11 21.7	−15 06 36	1.67	4.3		3C 196	08 09 58.9	48 22 09	4.93	14.3	
0112-017	01 12 43.4	−01 42 59	5.37	15.3		0830+112	08 30 35.5	11 15 30	3.43	7.7	
PG0117+213	01 17 34.6	21 18 05	4.85	18.6		3C 204	08 33 17.9	65 24 04	4.85	18.3	
PG0119+229	01 19 56.9	22 54 36	5.65	20.1		3C 205	08 35 09.9	58 04 53	4.34	20.8	
NGC 526A	01 21 37.2	−34 19 33	2.33	6.3		3C 206	08 37 27.9	−12 03 53	5.85	11.9	
3CR48	01 34 49.8	32 54 20	4.35	9.5		3C 207	08 38 01.9	13 23 05	5.40	14.1	
0205+024	02 05 14.5	02 28 41	2.99	8.3		PG0844+34	08 44 33.9	34 56 08	3.39	9.7	
MKN590	02 12 00.4	−00 59 58	3.07	8.7		3C 208	08 50 23.0	14 03 58	3.60	10.2	
NGC931	02 25 14.4	31 05 22	7.07	21.7		OJ 287	08 51 57.2	20 17 58	2.75	5.4	
0226-038	02 26 22.2	−03 50 55	2.37	6.5		3CR215	09 03 44.1	16 58 16	3.75	7.8	
PHL 1377	02 32 36.5	−04 15 09	2.29	6.0		0906+015	09 06 34.9	01 33 46	3.38	8.9	
0235+164	02 35 53.0	16 24 05	7.60	20.6		MKN 704	09 15 39.4	16 30 59	3.15	6.3	
PKS0237-233	02 37 52.5	−23 22 06	2.23	6.6		H0917-074	09 17 03.0	−07 22 57	3.30	7.8	
0241+622	02 41 01.2	62 15 29	73.30	73.8	1	0923+201	09 23 05.6	20 07 06	4.16	11.2	
H0323+022	03 23 38.0	02 14 47	8.68	24.8		PG0923+129	09 23 20.1	12 57 07	4.03	12.0	
NRAO 140	03 32 22.0	32 08 38	14.22	59.0	1	4C39.25	09 23 55.3	39 15 23	1.69	1.8	
H0414+009	04 14 18.0	00 58 03	9.15	26.9		PG0934+013	09 34 26.4	01 19 12	4.69	12.4	
3C 111	04 15 00.6	37 54 19	32.61	63.0	1	NGC 2992	09 43 17.4	−14 05 44	5.56	16.2	
0420-388	04 20 29.6	−38 51 42	1.91	5.8		PG1001+054	10 01 43.3	05 27 35	1.88	6.2	
0420-014	04 20 43.3	−01 27 24	9.43	39.2		1011+25	10 11 05.6	25 04 09	3.10	16.3	
3C120	04 30 31.6	05 14 58	12.32	56.0	1	1012+008	10 12 20.7	00 48 33	3.22	8.9	
3C 138	05 18 16.9	16 35 27	23.28	60.5	1	1020-103	10 20 04.0	−10 22 32	4.89	12.5	
PKS0521-365	05 21 12.8	−36 30 15	3.37	13.4		B2 1028+313	10 28 09.8	31 18 20	1.98	2.7	
0537-286	05 37 56.7	−28 41 26	1.95	3.6		3C245	10 40 05.9	12 19 16	2.70	8.1	
3C 147	05 38 43.0	49 49 45	21.64	45.1	1	3CR249.1	11 00 27.3	77 15 08	2.92	6.9	

© American Astronomical Society • Provided by the NASA Astrophysics Data System

1989AJ.....97..777E

TABLE I. (continued)

Object	R.A.	decl.	N_H^a	T_{peak}	Notes	Object	R.A.	decl.	N_H^a	T_{peak}	Notes
MKN 421	11 01 40.5	38 28 42	1.45	1.5		MKN290	15 34 45.3	58 04 00	2.32	3.4	
3C254	11 11 53.3	40 53 41	1.75	1.7		3CR323.1	15 45 31.0	21 01 28	4.04	11.5	
1115+080	11 15 41.4	08 02 25	3.61	10.4		1546+027	15 46 58.2	02 46 07	6.78	28.9	
PG1116+215	11 16 30.0	21 35 42	1.44	2.2		PG1552+085	15 52 19.0	08 31 08	3.47	11.2	
MKN734/PG	11 19 10.9	12 00 48	2.74	5.1		1611+343	16 11 47.8	34 20 21	1.44	3.4	
1121+422	11 21 52.0	42 16 52	2.33	5.2		TON256	16 12 08.5	26 11 47	3.77	12.6	
MKN180	11 33 29.9	70 24 60	1.27	1.5		MKN 876	16 13 36.2	65 50 37	2.66	3.3	
3C263	11 37 09.3	66 04 26	.82	1.3		MKN 877	16 17 56.7	17 31 34	4.35	14.0	
PG1138+040	11 38 42.4	04 03 39	1.87	3.5		3C334	16 18 06.9	17 43 31	4.22	13.4	
1146-037	11 46 23.8	−03 47 29	2.77	4.9		3C336	16 22 31.8	23 52 03	4.52	17.4	
NGC 4051	12 00 36.3	44 48 34	1.31	1.6		PG1630+377	16 30 15.1	37 44 11	.90	1.8	
GQ COMAE	12 02 08.9	28 10 54	1.72	2.6		1634+706	16 34 51.8	70 37 37	5.74	11.7	
PG1211+143	12 11 44.8	14 19 53	2.83	5.9		1635+119	16 35 26.0	11 55 40	4.29	11.7	
ON235	12 15 21.1	30 23 41	1.60	2.3		3C345	16 41 17.6	39 54 10	.74	1.8	
1217+023	12 17 38.3	02 20 20	1.97	4.5		MKN501	16 52 11.6	39 50 24	1.73	3.8	
1219+305	12 18 51.6	30 27 15	1.78	2.9		3C351	17 04 03.4	60 48 32	2.26	3.2	
MKN 205	12 19 33.7	75 35 17	2.74	5.0		1721+343	17 21 31.9	34 20 41	3.06	7.8	
1225+317	12 25 55.8	31 45 12	1.23	1.1		1725+044	17 25 56.0	04 29 29	7.03	29.2	
PG1229+204	12 29 32.9	20 26 03	2.58	6.7		I ZW 186	17 27 04.2	50 15 31	2.58	10.2	
NGC 4593	12 37 04.6	−05 04 15	1.97	4.4		PKS1739+17	17 39 26.7	17 21 59	5.44	20.8	
PG1241+176	12 41 40.8	17 37 26	1.93	7.5		1803+676	18 03 37.3	67 37 53	5.00	6.7	
PG1244+026	12 44 02.0	02 38 30	1.93	4.6		3C380	18 28 12.8	48 42 40	6.60	14.0	
3C277.1	12 50 14.9	56 50 38	1.03	1.1		NGC6814	19 39 55.5	−10 26 33	9.80	33.9	
1252+119	12 52 07.5	11 57 19	2.63	9.3		PKS2121+053	21 21 14.7	05 22 28	6.27	33.5	
3C279	12 53 35.7	−05 31 06	2.22	5.8		3C433	21 21 30.5	24 51 18	8.75	29.9	
MKN 231	12 54 04.9	57 08 36	1.03	1.3		2126-158	21 26 26.7	−15 51 48	4.85	22.0	
PG1307+085	13 07 16.1	08 35 48	2.20	6.3		2128-123	21 28 52.5	−12 20 20	4.83	10.2	
NGC 5033	13 11 09.1	36 51 29	1.00	1.9		IIZW136	21 30 01.1	09 54 59	4.20	8.5	
3C287	13 28 15.9	25 24 38	1.06	1.8		PKS2134+004	21 34 05.2	00 28 26	5.12	19.1	
3C286	13 28 49.9	30 45 58	1.14	2.2		PHL1657	21 35 01.1	−14 46 26	4.45	11.9	
1331+170	13 31 09.9	17 04 23	1.76	4.6		NGC 7172	21 59 07.2	−32 06 36	1.65	5.0	
MCG-6-30-15	13 33 01.8	−34 02 26	4.06	9.4		BL LAC	22 00 39.2	42 02 08	20.15	58.0	1
PG1333+176	13 33 36.5	17 40 31	1.76	4.7		2201+315	22 01 01.2	31 31 06	9.91	20.6	
3C288.1	13 40 29.8	60 36 49	2.09	2.8		PG2209+184	22 09 30.1	18 27 01	4.82	10.8	
IC4329A	13 46 27.8	−30 03 41	4.55	10.4		MKN304	22 14 45.2	13 59 26	5.23	14.7	
MKN 279	13 51 51.8	69 33 13	1.64	1.4		2216-038	22 16 15.9	−03 50 33	6.18	24.8	
PG1352+183	13 52 12.5	18 20 01	1.84	4.6		3C446	22 23 11.0	−05 12 16	5.26	18.9	
PG1352+011	13 52 25.7	01 06 51	2.10	6.1		CTA102	22 30 07.7	11 28 24	5.05	13.1	
PG1402+266	14 02 58.7	26 10 01	1.42	4.0		NGC7314	22 33 00.1	−26 18 31	1.45	5.3	
PG1404+226	14 04 02.7	22 37 59	2.00	6.4		MR2251-179	22 51 25.7	−17 50 54	2.84	6.0	
PG1407+265	14 07 07.6	26 32 29	1.38	3.3		3C354.3	22 51 29.4	15 52 55	7.13	14.4	
NGC 5506	14 10 39.1	−02 58 24	4.22	16.2		PKS2251+113	22 51 40.5	11 20 40	5.53	21.6	
PG1416-129	14 16 21.3	−12 56 59	7.20	21.1		PKS2254+023	22 54 44.4	02 27 15	5.88	22.2	
3C298	14 16 38.9	06 42 21	2.06	7.3		NGC7469	23 00 44.2	08 36 15	4.82	15.4	
PG1425+267	14 25 21.7	26 45 38	1.54	5.1		2304+042	23 04 30.0	04 16 40	5.52	16.1	2
PG1426+015	14 26 33.7	01 30 27	2.64	8.1		NGC7582	23 15 38.3	−42 38 31	1.48	4.3	
3C309.1	14 58 58.0	71 52 13	2.41	1.8		PKS2344+092	23 44 03.4	09 14 06	5.05	19.9	
PG1501+106	15 01 36.3	10 37 57	2.23	6.3		2345+184	23 45 56.7	18 27 29	4.25	15.8	
PG1519+226	15 19 02.0	22 38 22	3.88	19.1		MKN 541	23 53 28.0	07 14 36	5.02	17.7	

a. In units of 10^{20} atoms cm^{-2}; for an assumed T_{spin} of 250 K (see text)

1. Bright H I spectrum. Was not corrected for stray radiation (see text).
Opacity correction dominates over stray radiation correction in most cases.

2. Bell Labs survey was extraplated to correct this spectrum. Error may be larger than normal.

techniques for removing stray radiation, become unreliable. However, the brightness of the H I means also that stray radiation will be a relatively unimportant component of the total N_H and the "uncorrected" 140 ft spectra are thus fairly accurate. Sources so affected are flagged in Table I; the uncertainty in their N_H is dominated by the uncertain opacity correction. We also tabulate the peak brightness temperature (T_{peak}). The dominant error in the tabulated column densities may be due to either the baseline noise referred to above or to the uncertainty due to the opacity correction. Figure 4 shows how the uncertainty in N_H due to T_{spin}, $\Delta N_H(T_{spin})$ dominates above the measurement errors of 1×10^{19} atoms cm^{-2} (dashed line) for $N_H \gtrsim 4\times10^{20}$ atoms cm^{-2}. If the area under Galactic H I profiles could always be measured to ~2%, then opacity-correction uncertainties would dominate at all values of N_H.

Figures 5(a) and 5(b) compare the optically thin 140 ft and Bell values of N_H as both a ratio and a difference as a function of N_H (140 ft). The ratio of 140 ft/Bell stays constant with N_H, while the difference seems to grow slightly. This suggests that small-scale structure is a constant fraction of the total. That is, at high latitudes the Galactic N_H in a 21′ field is equal to that in the 3°×2° Bell fields with a 1σ uncertainty of 11% on average.

III. CONCLUSIONS

The values of N_H tabulated here have typical uncertainties of ~10^{19} atoms cm^{-2} and so are about ten times more accurate than column densities derived from the Bell Labs survey alone. It is worth noting here that for the purposes of investigating small amounts of x-ray absorption it is the col-

© American Astronomical Society • Provided by the NASA Astrophysics Data System

1989AJ.....97..777E

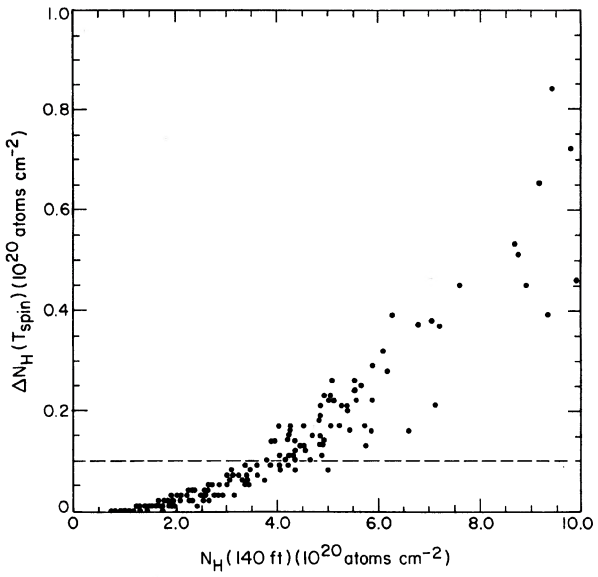

FIG. 4. Percentage error in N_H due to opacity uncertainties (T_{spin}) as a function of N_H (140 ft). The horizontal line is the uncertainty due to other effects. Opacity uncertainties dominate above about 4×10^{20} atoms cm^{-2}.

umn density due to hydrogen and helium alone that contributes to the photoelectric cross section in the C band below 0.28 keV (Morrison and McCammon 1983). Hydrogen in any form other than atomic appears to be uncommon at high Galactic latitudes (Blitz, Magnani, and Mundy 1984) so that the 21 cm data give an unusually direct and clean means of determining the column that must absorb x rays.

The extreme x-ray–ultraviolet telescopes on *ROSAT* (Pye 1984) and *EUVE* (Bowyer 1987) can only detect extragalactic sources if they lie in directions of unusually small Galactic column density. There are two AGN in Table I with N_H below 0.9×10^{20} atoms cm^{-2} and seven with N_H below 1.1×10^{20} atoms cm^{-2}. These low N_H AGN will make good targets for the extreme x-ray–ultraviolet telescopes. Our nearly 200 AGN form an essentially random sample of the high-latitude sky. We can estimate then that roughly 1% of the sky has column densities of 0.9×10^{20} atoms cm^{-2} or less.

The need for more accurate column densities will rise rapidly with the many soft-x-ray sources that are expected to be discovered with the soft-x-ray sky-survey satellite *ROSAT* (Trümper 1984, due for launch in February 1990). The effects of uncertain Galactic N_H can be important to log N–log S studies and hence to questions of quasar evolution and the origin of the x-ray background (Zamorani *et al.* 1988). An all-sky survey of Galactic N_H with a beam size similar to that used here and free of stray radiation would substantially reduce these problems and would be of great utility for x-ray astronomy.

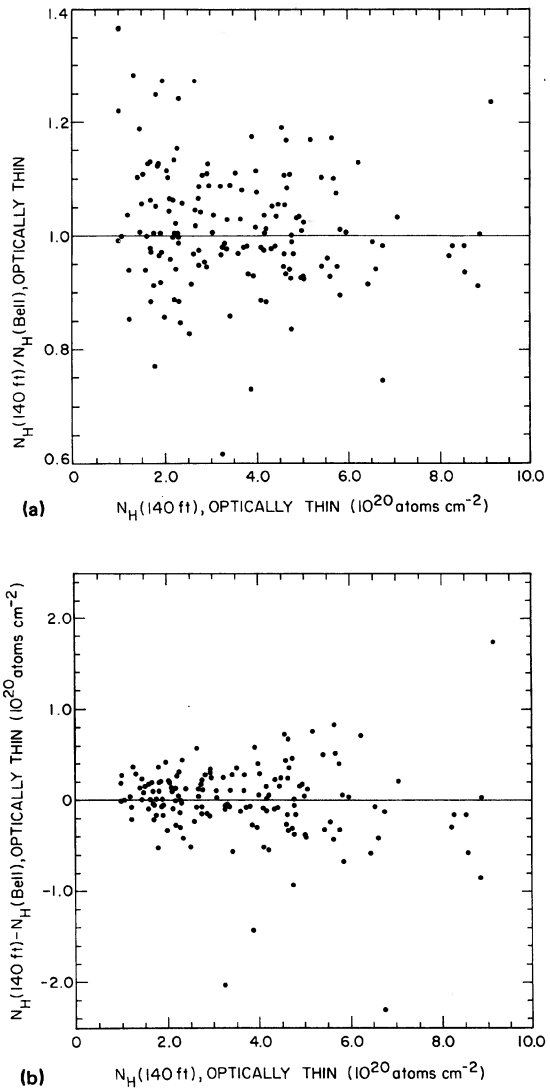

FIG. 5. Ratio (a) and difference (b) between N_H (140 ft) and N_H (Bell) as a function of N_H (140 ft) in units of 10^{20} atoms cm^{-2}.

This work was supported in part by NASA contract No. NAS8-30751, and by NASA Astrophysics Data Program grant No. NAG8-689.

REFERENCES

Blitz, L., Magnani, L., and Mundy, L. (1984). Astrophys. J. Lett. **282**, L9.
Bowyer, S. (1986). Adv. Space Res. **6**, 153.
Branduardi-Raymont, G., *et al.* (1987). Lect. Not. Phys. **266**, 407.
Brunner, H., *et al.* (1988). In preparation.
Dickey, J. M. (1988). In *QSO Absorption Lines: Probing the Universe,* edited by J. C. Blades, D. Turnshek, and C. A. Norman (Cambridge University, Cambridge), p. 254.
Dickey, J. M., and Benson, J. M. (1982). Astron. J. **87**, 278.
Elvis, M., Green, R. F., Bechtold, J., Schmidt, M., Neugebauer, G., Soifer, B. T., Matthews, K., and Fabbiano, G. (1986). Astrophys. J. **310**, 291.
Giacconi, R., *et al.* (1979). Astrophys. J. **230**, 540.
Giommi, P., and Tagliaferri, G. (1987). *Observational Cosmology,* IAU Symposium No. 124, edited by G. Burbidge (Reidel, Dordrecht), p. 601.
Gorenstein, P., Harnden, R. F., and Fabricant, D. (1981). IEEE Trans. Nucl. Sci. **NS-28**, 869.
Lockman, F. J., and Dickey, J. (1989). Annu. Rev. Astron. Astrophys. (in

© American Astronomical Society • Provided by the NASA Astrophysics Data System

1989AJ.....97..777E

press).
Lockman, F. J., Jahoda, K., and McCammon, D. (1986). Astrophys. J. **302**, 432.
Madejski, G. (1985). Ph.D. thesis, Harvard University.
Marshall, H. L., Avni, Y., Braccesi, A., Huchra, J. P., Tananbaum, H., Zamorani, G., and Zitelli, V. (1984). Astrophys. J. **283**, 50.
McCammon, D., Burrows, D. N., Sanders, W. T., and Kraushaar, W. L. (1983). Astrophys. J. **269**, 107.
Morrison, R., and McCammon, D. (1983). Astrophys. J. **270**, 119.
Piccinotti, G., Mushotzky, R. F., Boldt, E. A., Holt, S. S., Marshall, E. E., Serlemitsos, P. J., and Shafer, R. A. (1982). Astrophys. J. **253**, 485.
Pye, J. P. (1984). In *X-ray and UV Emission from Active Galactic Nuclei*, edited by Brinkmann and J. Trümper (MPE, Garching), p. 261.
Stark, A. A., Heiles, C., Bally, J., and Linke, R. (1984). Bell Labs, privately distributed magnetic tape.
Sternberg, J. R., White, N. E., Barr, P., and Osborne, L. (1986). *The EXOSAT Observing Log* (ESTEC, Noordwijk).
Taylor, B. G., Anderson, R. D., Peacock, A., and Zobl, R. (1981). Space Sci. Rev. **30**, 479.
Trümper, J. (1984). In *X-ray and UV Emission from Active Galactic Nuclei*, edited by Brinkmann and J. Trümper (MPE, Garching), p. 254.
Wilkes, B. J., and Elvis, M. (1987). Astrophys. J. **323**, 243.
Zamorani, G., Gioia, I. M., Maccacaro, T., and Wolter, A. (1988). Astron. Astrophys. **196**, 39.

© American Astronomical Society • Provided by the NASA Astrophysics Data System